

INCONSISTENCIES BETWEEN DIFFERENT ACCELERATED TEST METHODS USED TO ASSESS ALKALI-AGGREGATE REACTIVITY

Andreas Leemann^{1,*}, Jean-Gabriel Hammerschlag², Cédric Thalmann³

¹EMPA (Swiss Federal Laboratories for Materials Testing and Research), Überlandstr. 129, CH-8600 DÜBENDORE, Switzerland

²Holcim, CH-1312 ECLÉPENS, Switzerland

³B-I-G Büro für Ingenieurgeologie AG, Dorfstrasse 10, CH-3073 GÜMLIGEN, Switzerland

Abstract

In the prevention of damage due to alkali-aggregate-reaction accelerated test methods are an indispensable tool to assess the potential reactivity of aggregates and concrete. However, the interpretation of the test results is often not definite. In Switzerland an accelerated microbar test and a concrete performance test are used to characterize the potential reactivity of aggregates and concrete. Sometimes the results obtained with the two tests are inconsistent. The goal of this study is to identify the reason for such inconsistencies. Two aggregates from alluvial deposits are selected. Both aggregates indicate a potential reactivity in the microbar test. However, only the concrete mixtures produced with aggregate A expand substantially. The microstructural study shows that sandstone as main siliceous constituent of aggregate B is substantially dissolved in the microbars but displays only occasional reactivity in the concrete whereas aggregate A exhibits dissolution and precipitation phenomena in microbars and concrete.

Keywords: alkali-aggregate-reaction, prevention, accelerated test methods, inconsistencies

1 INTRODUCTION

In Switzerland, the first case of alkali-aggregate reaction (AAR) was published in 1995 [1]. In recent years, an increasing number of cases has been reported [2-5]. Consequently, recommendations in order to prevent AAR in new structures have been published [5,6]. In the prevention of AAR, accelerated test methods are an indispensable tool to assess the potential reactivity of aggregates and concrete. In Switzerland, an accelerated microbar test [7] and a concrete performance test [8] are used. However, with the growing data base, it has been becoming obvious that inconsistencies exist in the results of these two test methods; aggregates with high expansion rates in the microbar test show low expansion rates in the concrete performance test. As a wide variety of concrete mix designs was usually used, this phenomenon has not been sufficiently verified so far. To complicate matters, there is a great diversity of aggregates including various sediments and igneous rocks in different states of metamorphosis used for concrete production.

The goal of the project is to verify the supposed inconsistencies between the results obtained with the two test methods and to identify some rock types responsible for such inconsistencies. Two potentially reactive aggregates from different regions of Switzerland are chosen; aggregate A containing mainly metamorphic rocks, aggregate B containing mainly sediments. The field performance of aggregate A shows that it can cause severe damages in concrete structures. The potential reactivity of aggregates and of concrete mixtures is measured. Additionally, mortar bars and concrete prisms are studied using an environmental scanning electron microscope in order to identify reactive rocks and minerals.

2 MATERIALS AND METHODS

2.1 Materials and mix design

To produce the concrete, an ordinary Portland cement CEM I 42.5 N with a Na₂O-equivalent of 0.89 % was used in three different dosages (Tables 1 and 2). Both aggregates were extracted from alluvial deposits and are well rounded. The quarry of aggregate A is located in the central Alps of Switzerland, the one of aggregate B in the Swiss middle land. In order to achieve good workability, a

* Correspondence to: andreas.leemann@empa.ch

superplasticizer based on polycarboxylate ether was used (Na_2O -equivalent of 0.38%).

2.2 Methods for analysis

The petrography of the aggregates was determined according to Swiss standard SN 670'115 [9]. For thermogravimetric analysis (TGA) and X-ray diffraction analysis (XRD), the samples of aggregate A and B were ground < 0.063 mm. TGA was carried out in N_2 on about 10 mg of sample at 20°C up to 980°C with a temperature increase of $20^\circ\text{C}/\text{min}$ (Mettler-Toledo TGA/SDTA 851). XRD was performed using a Panalytical X'Pert Pro powder diffractometer in a 2θ -range of 5 - 80° .

The potential reactivity of the aggregates was measured with the microbar test according to [7]. In this test, the expansion of mortar bars is used to classify aggregates as non-reactive or potentially reactive. First, the aggregates are crushed and sieved to a grain size fraction of 16 - $63\ \mu\text{m}$. Afterwards, mortar bars ($1\ \text{x}\ 1\ \text{x}\ 4\ \text{cm}$) with a ratio of cement to aggregate of 2, 5 and 10 are produced. The Na_2O -equivalent of the cement is increased to 1.5 % by adding NaOH. The curing includes a treatment in a 10 % KOH solution at 150°C for six hours. The highest mean expansion of the microbars with different cement to aggregate ratios is used to classify the aggregate. An aggregate is classified as potentially reactive when the expansion is $\geq 0.11\ \%$. The microbar test shows a good correlation to the NBRI test [10,11]. The microbar test was conducted on four different grain size fractions of the aggregates: 0-4 mm, 4-8 mm, 8-16 mm and 16-32 mm.

The potential reactivity of the concrete was measured according to [8]. In this test, three prisms ($7\ \text{x}\ 7\ \text{x}\ 28\ \text{cm}$) are exposed to 60°C and 100 % relative humidity for 20 weeks. The Na_2O -equivalent of the cement is increased by a NaOH addition. The amount of added NaOH is the difference between the highest possible Na_2O -equivalent of the cement used based on its standard deviation during production and the actual Na_2O -equivalent present. However, no NaOH was added in the present study in order to prevent an influence on cement hydration. When the expansion exceeds 0.02 % after 20 weeks, the concrete is classified as potentially reactive.

Microbars and concrete prisms were studied with an environmental scanning electron microscope (ESEM-FEG XL30) in order to identify reactive minerals and aggregates. The operating condition of the ESEM was 15 kV in the high vacuum mode using a back scatter detector. The chemical composition of aggregates and minerals was analyzed with energy dispersive X-ray spectroscopy (EDX) using point spectra. An EDAX 194 UTW detector, a Philips digital controller and Genesis Spectrum Software (Version 4.6.1) with ZAF corrections were used.

As the microbars used to determine the potential reactivity of the aggregates were not available any more, aggregates from a second batch originating from the same quarries had to be used for the microstructural analysis. Four microbars (cement/aggregate ratio = 2, grain size fraction 0/4 mm and 8/16 mm, respectively) of aggregate A and B were dried for three days at 50°C , impregnated with epoxy resin, cut in longitudinal direction, polished and carbon coated. The images taken display grey scale values from 0 to 255. They have dimensions of $\sim 1.9\ \text{x}\ 2.5\ \text{mm}$ and a resolution of $968\ \text{x}\ 1420$ pixels (pixel dimension: $1.9\ \text{x}\ 1.7\ \mu\text{m}$). 16 images were made per prism resulting in 64 images per aggregate which corresponds to $\sim 300\ \text{mm}^2$ of analyzed area. The approach used to quantify the degree of reactivity is similar to the one chosen by Ben Haha et al. [12]. Because dissolved minerals leave cavities and are filled with epoxy by impregnation, they appear as dark areas in the BSE images. As a result, they can be analyzed by a segmentation based on grey scale values. Areas with grey scale values from 0 to 80 were separated representing dissolved minerals, air voids, capillary pores and cracks. Air voids and cracks are defined as "background", dissolved minerals and capillary pores as "dissolved minerals". The magnification for the images was chosen in a way that the majority of the capillary pores have a diameter of two pixels or smaller. As a result, it was possible to eliminate the majority of the capillary pores present in the class "dissolved minerals" by applying an erosion function with a width of one pixel. Some background noise of capillary pores remains though. Applying this step, the areas of dissolved minerals are decreased by the width of one pixel as well. As a result, the area of effectively dissolved minerals is underestimated by 10-15% like detailed analysis of four images revealed. However, no correction factor was applied. The analyzed area of "dissolved minerals" is equal to its volume fraction if the microbars are assumed to be isotropic. Because the volume percentage of aggregates in the microbars is known due to the mix design, the amount of reacted aggregates can be calculated. An example of a BSE-image and its segmentation are shown in Figures 1 and 2. The software used for this image analysis has been developed on a Matlab 6.5 environment.

After conducting the concrete performance test, one prism of concrete C-A3 and C-B3 were selected in order to qualitatively identify reactive minerals and aggregates. A core with a diameter of 50 mm was taken from the middle section of the prisms. Five discs (diameter 50 mm, height 20 mm)

were cut per core and dried for three days at 50°C. After drying, they were impregnated with epoxy resin, polished and carbon coated. The operating conditions for the ESEM correspond to the ones used for the analysis of the microbars.

3 RESULTS

3.1 Petrography

Aggregate A mainly consists of metamorphic and igneous rocks, gneiss being the most frequent rock type (Table 3). In contrast, aggregate B mainly consists of sediments dominated by sandstone and limestone (Table 4). Aggregate A contains quartz, albite, orthoclase, muscovite, calcite, clinocllore, cordierite and dolomite (listed in order of decreasing concentration). The calcite content determined is 6.9 weight-%. In aggregate B calcite, quartz and albite are present (listed in order of decreasing concentration) with traces of dolomite, orthoclase, muscovite, clinocllore, illite and ferrian. The calcite content is 63.3 weight-%. Assessed qualitatively in BSE images, there is no substantial difference between the size of quartz minerals present in gneiss and granite of aggregate A and the one in sandstone of aggregate B.

3.2 Microbar test

Both aggregates exceed the limit value of 0.11 % and can therefore be classified as potentially reactive (Figure 3). There are some minor differences in the expansion of the different grain size fraction. However, the difference between aggregate A and B is substantial; the microbars produced with aggregate B expand more than twice as much as the ones produced with aggregate A. Microbars produced with the second batch of aggregate A display an expansion of 0.169 (0-4 mm) and 0.160 % (8-16 mm), the ones produced with the second batch of aggregate B lead to values of 0.237 (0-4 mm) and 0.248 % (8-16 mm).

3.3 Concrete performance test

Concrete produced with aggregate A shows an almost linear expansion with time (Figure 4). The mixtures containing 300 and 350 kg/m³ of cement reach about the same value of expansion after 20 weeks. Concrete C-A3 with 400 kg/m³ of cement exceeds the limit value of 0.02 % and has to be classified as potentially reactive.

The expansion rates of concrete mixtures produced with aggregate B are very low and considerably differ from the ones of concrete C-A1 to C-A3. As a result, there is no relation between expansion and cement content.

3.4 Reactive aggregates and minerals

In the microbars produced with aggregate A mainly gneiss and granite show dissolution features. Occasionally, there are partly dissolved minerals present in the sediments. Some dissolution phenomena are present in feldspars, but the most frequently dissolved mineral is quartz (Figures 5 and 6). Typically dissolution starts at the grain boundaries of quartz. In the microbars produced with sand 0/4 mm the volume of dissolved minerals is 2.4 %, in the microbars produced with gravel 8/16 mm it is 2.0 %. These values translate to 10.6 and 8.8 % of dissolved minerals present in the aggregates.

In the microbars produced with aggregate B, sandstones exhibits most of the dissolution features. Minerals in quartzite and siliceous limestone get dissolved as well, but these rocks are present in lower quantities. Like in gneiss and granite, quartz is dissolved from its grain boundaries inwards (Figure 7). In calcareous sandstones often honey-comb structured minerals are present in areas with large amounts of minerals dissolved (Figure 8). EDX analysis shows silicon, calcium, aluminum and potassium as main constituents (listed in order of decreasing concentration) identifying them as phyllosilicates. The microbars produced with sand and gravel show 1.4 and 1.6 % of dissolved minerals. This equates to 6.2 and 7.0 % of dissolved minerals in the aggregates.

In concrete C-A3 there are reactive gneiss (Figure 9), granite and limestone containing detritic quartz. Gneiss is the most reactive aggregate. The only mineral clearly showing dissolution features is quartz (Figure 10). There are gel deposits in cracks within the aggregates and in pores along the aggregates.

In concrete C-B3 there is considerably less gel formation than in concrete C-A3 (Figures 11 and 12).

4 DISCUSSION

The results of the two accelerated test methods are contradictory; aggregate A shows a moderate expansion in the microbar test but reaches the limit in the concrete performance test while

aggregate B is highly reactive in the microbar test and non-reactive in the concrete performance test. These differences must have a relation to the characteristics of the quartz present.

In general, the solubility of quartz increases with increasing pH and temperature and can be further enhanced by the presence of certain cations [13-15]. But little data exist about the solubility of quartz in alkaline solutions with a composition similar to the pore solution of concrete where mainly potassium, sodium and calcium cations are present. However, the conditions during the test were identical for both aggregates. Concluding from the expansion measurements and microstructural analysis, it is obvious that the thermodynamic stability and the dissolution kinetics of quartz present in aggregate B are different to the one in aggregate A. Quartz in aggregate B dissolves under the conditions present in the microbar test but is more or less stable in the conditions present in the concrete performance test. In contrast, quartz in aggregate A dissolves in both tests. This behavior must be the result of differences in the crystal structure of the quartz resulting from differences in the geological history of the aggregates. Aggregate A was subjected to a retrograde metamorphism of the greenschist facies while the majority of the rock types present in aggregate B are not metamorphic. It has been shown that the reactivity of quartz in concrete increases with increasing degree of deformation [16,17]. Other characteristic of quartz like grain size, shape of mineral boundaries, twin formations or presence of substitutable ions like iron or aluminum have the potential to influence its reactivity [18-20]. Moreover, assemblages of different minerals in the aggregates might have an influence as well. Sandstone can react even stronger than chert due to the catalytic effect of coexisting minerals [21]. However, reactive minerals containing aluminum may have a mitigating influence on AAR as aluminum hydroxides in solution slow down the dissolution of quartz at pH10-13 and elevated temperatures considerably [22]. As clay minerals containing aluminum hydroxide are present in aggregate B the solubility of quartz might have been influenced accordingly.

Clay minerals are often the reason for swelling in sedimentary rocks and soils. However, the high expansion rates in the microbar test obtained with aggregate B can most likely not be attributed to the phyllosilicates present as swelling decreases with increasing ionic strength of the aqueous solution [23]. Moreover, clay minerals start to dissolve at high pH causing a decrease of swelling pressure [24].

The volume of dissolved minerals determined in the microstructural analysis does not correlate with the expansion measured in the microbar test. The expansion of the microbars produced with aggregate A is lower compared to aggregate B, although the first shows a higher amount of dissolved minerals. The reason for this inconsistency might be the relatively high degree of reaction shown by both aggregates. The expansion rates of mortar bars and concrete prisms in accelerated tests show a linear correlation with the amount of dissolved minerals up to about 0.3 % of dissolved minerals [12]. At a higher degree of dissolution, a non-linear behavior results to the development of cracks. As the degree of reaction in the microbar test with values of 8.8-10.6 % for aggregate A and 6.2-7.0 % for aggregate B is significantly higher than 0.3 %, no linear correlation between amount of dissolved minerals and expansion can be expected. Furthermore, the tensile strength of the aggregates used has an influence as well. Presumably, certain sandstone aggregates present in aggregate B expand considerably leading to high microbar expansion and a relatively low amount of dissolved minerals.

Assessed qualitatively, the number of dissolution features and gel formations present in the concrete mixtures correlates with the measured expansion.

The linear increase of expansion shown by concrete C-A1 to C-A3 up to the age of 20 weeks indicates that a prolongation of the test would be sensible for such slow reacting aggregates.

The comparability of accelerated test methods and their meaningfulness have been the subject of various studies [e.g. 25-27]. Nevertheless, when the results of both accelerated test methods used in this study are compared with the number and location of structures affected by AAR in Switzerland, it becomes obvious that the results of the concrete performance test show a considerably better correlation than the ones of the microbar test. Most of the structures affected by AAR are located in the Alpine regions where mainly igneous and metamorphic rocks are used as aggregates [5]. However, in areas where sediments with often high expansion values in the microbar test are used as aggregates, the number of affected structures is particularly low. This observation has two implications for AAR prevention. Firstly, the condition of existing concrete structures produced with a specific aggregate has to be taken in account in the assessment of an aggregate classified with accelerates tests [6]. Secondly, it seems reasonable to do without the microbar test and use a method based on the concrete performance test to assess the potential reactivity of aggregates. As an example, a concrete producer could use a cement content that corresponds to the maximum content of any concrete mixture in his range to assess the reactivity of the aggregates he uses. Thereby, he gets information about the reactivity of his aggregates, and at the same time, he is in the position to assess the potential reactivity

of other concrete mixtures in his range. Nevertheless, the inconsistencies between microbar and concrete performance test have to be taken into account preparing the upcoming Swiss standard.

5 CONCLUSION

Thermodynamic stability and dissolution kinetics of quartz can differ depending on its geological history. As a result, aggregates of different origin and with different geological backgrounds can lead to inconsistent results in accelerated test with differing alkalinity and temperature. The observed inconsistencies seem to be caused by sandstone that is reactive in the conditions present in the microbar test but shows only no reactivity in the concrete performance test. The current data base does not permit to identify the reason for the difference in the reactivity of quartz observed in the used aggregates.

There is no correlation between the amount of reacted minerals and the expansion of microbars at the degree of reaction exhibited by the investigated aggregates due to the development of cracks.

Because the comparison of the results of the two accelerated tests with the distribution and frequency of AAR affected structures in Switzerland indicates a poor correlation with the microbar test and a considerably better correlation with the concrete performance test, the use of the microbar test seems questionable.

6 REFERENCES

- [1] Regamey, JM, and Hammerschlag, JG (1995): Barrage d'Ilsee - assainment. Research and Development in the Field of Dams, Proceedings of the ICOLD-Symposium (Crans-Montana, Switzerland).
- [2] Leemann, A, Thalmann, C, and Kruse, M (1999): Gebrochene Gesteinskörnungen. Schweizer Ingenieur- und Architektenverein, *SI+A* (24): 4-8.
- [3] Thalmann, C, Zingg, J, Rytz, G, Strahm, K, and Wyss C (2001): Verhinderung von betonschäden infolge Alkali-Aggregat-Reaktion. Schweizer Ingenieur- und Architektenverein, *tec* 21 (15): 2-8.
- [4] Leemann, A, Thalmann, C, and Studer, W (2005): Alkali-aggregate reaction in Swiss tunnels, *Materials and Structures* (38): 381-386.
- [5] Merz, C, Hunkeler, F, and Griesser, A (2006): Schäden durch Alkali-Aggregat-Reaktion an Betonbauten in der Schweiz. UWEK, Forschungsauftrag AGB2001/471, Bericht Nr. 599, Bern.
- [6] Frenzer, G, Hammerschlag, JG, Henoch, T, Leemann, A, Lunk, P, Pilloud, C, Rytz, G, Romer, M, Spicher, G, Thalmann, C, and Widmer, H (2005): Alkali-Aggregat-Reaktion (AAR) in der Schweiz, *cemsuisse*, Bern.
- [7] AFNOR P18-588 (1991): Granulats - stabilité dimensionnelle en milieu alcalin (essai accéléré sur mortier MICROBAR). Association Française de Normalisation, Paris.
- [8] AFNOR P18-454 (2004): Réactivité d'une formule de béton vis-à-vis de l'alcali-réaction (essai de performance). Association Française de Normalisation, Paris.
- [9] SN 670'115 (2005): Gesteinskörnungen: qualitative und quantitative Mineralogie und Petrographie. Swiss Standard, VSS Zürich.
- [10] SABS 1245 (1994): Potential reactivity of aggregates with alkalis (accelerated mortar prism method), South African Bureau of Standards, South Africa.
- [11] Hammerschlag, JG, and Zraggen, P, (2000): Beurteilung der Alkali-Zuschlag-Reaktion der Zuschläge und einzelner Betonrezepturen für die Alptransit Tunnelprojekte Gotthard und Lötschberg. TFB-Bericht, Projekt 998055, Ref. 05.001/2.
- [12] Ben Haha, M, Galluci, E, Guidoum, A, and Scrivener, KL (2007): Relation of expansion due to alkali silica reaction to the degree of reaction measured by SEM image analysis. *Cement and Concrete Research* (37) 1206-1214.
- [13] Dove, PM (1994): The dissolution kinetics of quartz in sodium chloride solutions at 25° to 300 °C. *American Journal of Science* 294, 665-712.
- [14] Dove, PM, and Christopher, JN (1997): The influence of the alkaline earth cations, magnesium, calcium, and barium on the dissolution kinetics of quartz. *Geochimica et Cosmochimica Acta* (61): 3329-3340.
- [15] Dove, PM (1999): The dissolution kinetics of quartz in aqueous mixed cation solutions. *Geochimica et Cosmochimica Acta*, (63): 3715-3727.
- [16] Monteiro, PJM, Shomglin, K, Wenk, HR, and Hasparyk, NP (2001): Effect of aggregate deformation on alkali-silica reaction. *ACI Materials Journal* (98): 179-83.

- [17] Kerrick, DM, and Hooton, RD (1992): ASR of concrete aggregate quarried from a fault zone - results and petrographic interpretation of accelerated mortar bar tests. *Cement and Concrete Research* (22): 949-960.
- [18] Glasser, FP (1992): Chemistry of alkali-aggregate reaction. In: Swamy RN (editor): *The alkali-silica reaction in concrete*. Blackie, London/Glasgow: 30-53.
- [19] Dove, PM (1995): Kinetic and thermodynamic controls on silica reactivity in weathering environments. In: White AF, Brantley SL (editors): *Chemical weathering rates of silica minerals*. *Reviews in Mineralogy* (31) Washington (DC): mineralogical Society of America: 235-290.
- [20] Broekmans, MATM (2004): Structural properties of quartz and their potential role for ASR. *Materials characterization* (53): 129-140.
- [21] Broekmans, MATM, and Jansen, J.B.H. (1998): Silica dissolution in impure sandstone: application to concrete. *Journal of Geochemical Exploration* (62): 311-318.
- [22] Bickmore, BR, Nagy, KL, Gray, AK, and Brinkerhoff, AR (2006): The effect of Al(OH)₄⁻ on the dissolution rate of quartz. *Geochimica et Cosmochimica Acta* (70): 290-305.
- [23] Xie, M, Moog, HC, and Kolditz, O (2007): Geochemical effects on swelling pressure of highly compacted bentonite: experiments and model analysis. In: *Theoretical and numerical unsaturated soil mechanics*, Springer Proceedings Physics (113) Berlin/Heidelberg.
- [24] Karnland, O, Olsson, S, Nilsson, U, and Sellin, P (2007): Experimentally determined swelling pressure and geochemical interactions of compacted Wyoming bentonite with highly alkaline solutions. *Physics and Chemistry of the Earth* (32): 275-286.
- [25] Grattan, PE (1997): A critical review of ultra-accelerated tests for alkali-silica reactivity. *Cement and Concrete Composites* (19): 403-414.
- [26] Wigum, BJ, French, WJ, Howarth, RJ, and Hills, C (1997): Accelerated tests for assessing the potential exhibited by concrete aggregates for alkali-aggregate reaction. *Cement and Concrete Composites* (19): 451-476.
- [27] Thomas, M, Fournier, B, Folliard, K, Ideker, J, Shehata, M (2006): Test methods for evaluating preventive measures for controlling expansion due to alkali-silica reaction in concrete. *Cement and Concrete Research* (36): 1842-1856.

Table 1: Composition of CEM I 42.5 N used in the concrete tests in weight-%.

SiO ₂	Al ₂ O ₃	Fe ₂ O ₃	CaO	MgO	SO ₃	K ₂ O	Na ₂ O	Mn ₂ O ₃	TiO ₂	P ₂ O ₅	SrO	Cl	Na ₂ O-equ	loss on ignition	Blaine [cm ² /g]
20.87	4.53	2.64	63.29	1.74	2.87	1.08	0.19	0.06	0.23	0.38	0.08	0.03	0.894	2.49	2.49

Table 2: Mix design of the concrete mixtures.

concrete mixture	C-A1	C-A2	C-A3	C-B1	C-B2	C-B3
aggregate type	A	A	A	B	B	B
aggregate [kg/m ³]	1920	1850	1800	1920	1850	1800
0/4 mm [%]	40	40	40	40	40	40
4/8 mm [%]	6	6	6	6	6	6
8/16 mm [%]	22	22	22	22	22	22
16/25 mm [%]	32	32	32	32	32	32
CEM I 42.5 N [kg/m ³]	300	350	400	300	350	400
SP [kg/m ³]	1.8	2.8	4.0	1.8	2.8	4.0
w/c	0.55	0.50	0.45	0.55	0.50	0.45

Table 3: Petrography of aggregate A.

rock types [weight-%]	grain size [mm]			
	1/4	4/8	8/16	16/25
fine grained gneiss	63	62	64	61
strongly foliated gneiss	7	6	8	5
granite	10	12	17	22
quartzite	4	2	2	4
limestone	16	18	9	8

Table 4: Petrography of aggregate B.

rock types [weight-%]	grain size [mm]			
	1/4	4/8	8/16	16/25
quartzite	8	3	4	2
igneous rocks	1	1	2	2
sandstone	46	31	24	30
dark limestone	8	12	17	11
bright limestone	34	52	50	52
porous sandstone and limestone	3	1	3	2
porous conglomerate	0	0	0	1

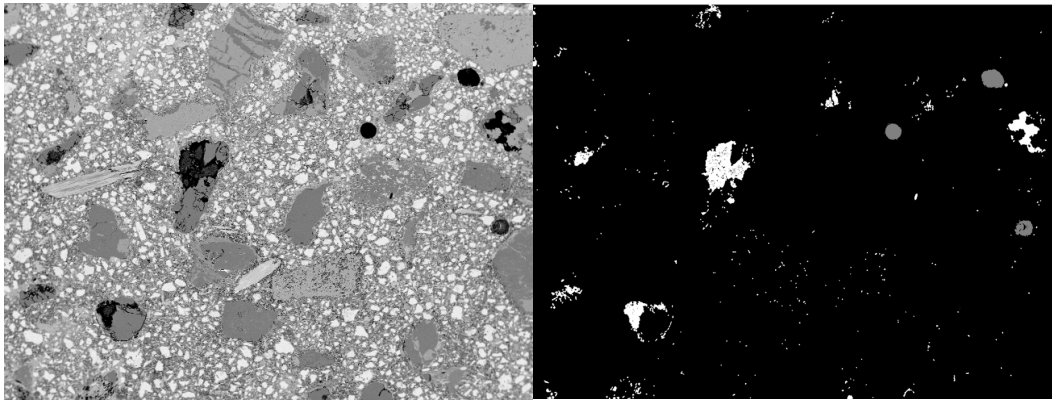


Figure 1 and 2: Backscattering electron image (left) and its segmentation in classes (right): "dissolved minerals" (white), "background" (grey) and "unspecified" (black). Length of base: 2.5 mm.

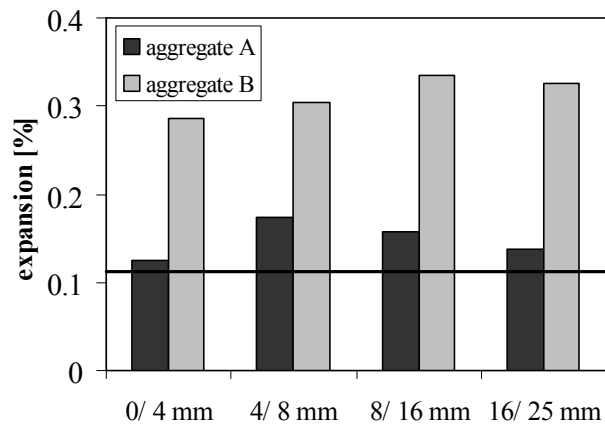


Figure 3: Microbar expansion of four different grain size fractions of aggregate A and B (expansion \geq 0.11% = potentially reactive).

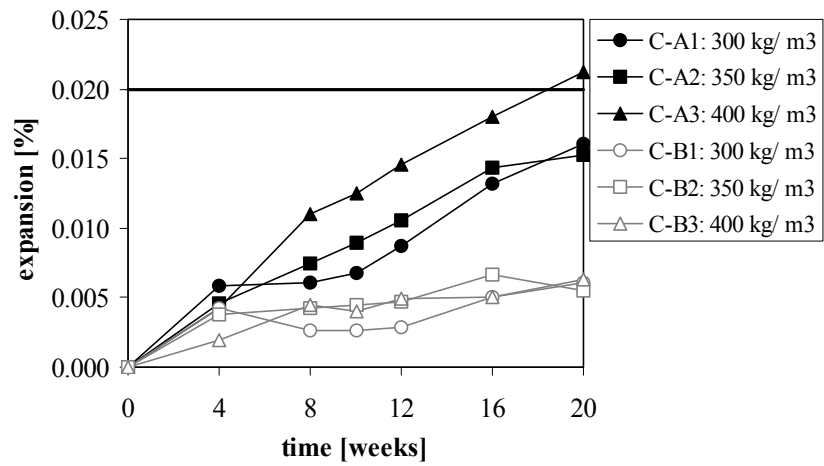


Figure 4: Expansion of concrete versus time (expansion $\geq 0.02\%$ = potentially reactive).

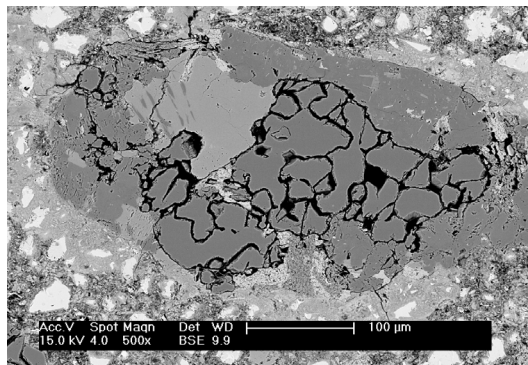


Figure 5: Gneiss with partly dissolved quartz. Microbar produced with aggregate A.

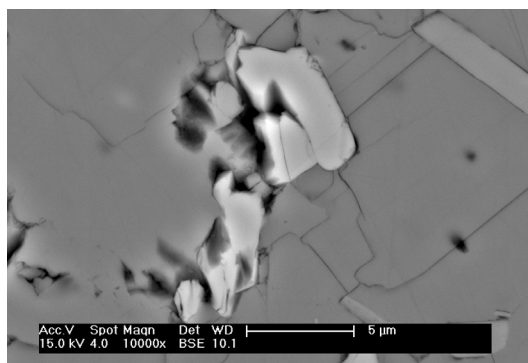


Figure 6: Feldspars (Anorthite: bright grey, albite: darker grey) with dissolution features. Microbar produced with aggregate A.

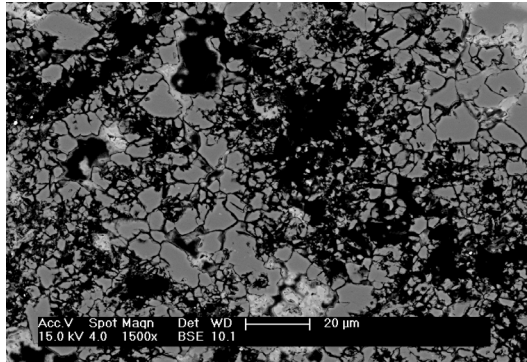


Figure 7: Partly dissolved quartz in sandstone. Microbar produced with aggregate B.

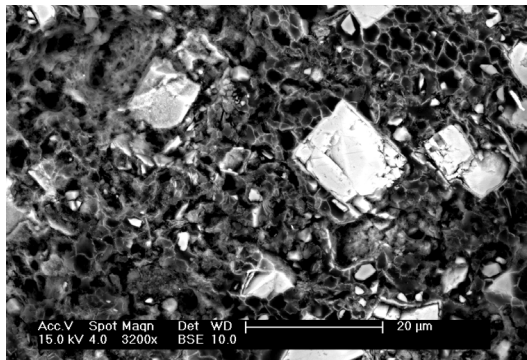


Figure 8: Calcareous sandstone with idiomorphic calcite and honey-comb structured phyllosilicates in cavity caused by the dissolution of quartz. Microbar produced with aggregate B.

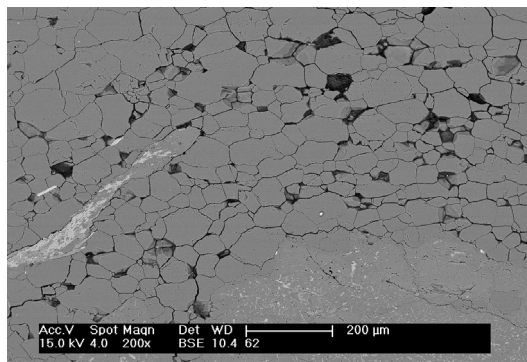


Figure 9: Quartz in gneiss aggregate cracked along its grain boundaries. Concrete produced with aggregate A.

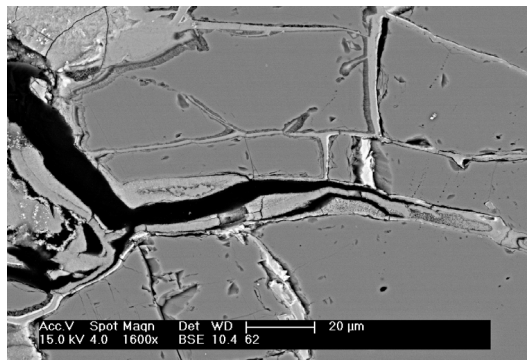


Figure 10: Quartz in gneiss with dissolution features and gel-filled cracks. Concrete produced with aggregate A.

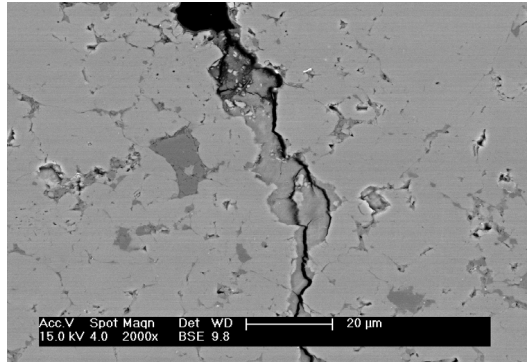


Figure 11: Gel filled crack in siliceous limestone. Concrete produced with aggregate B.

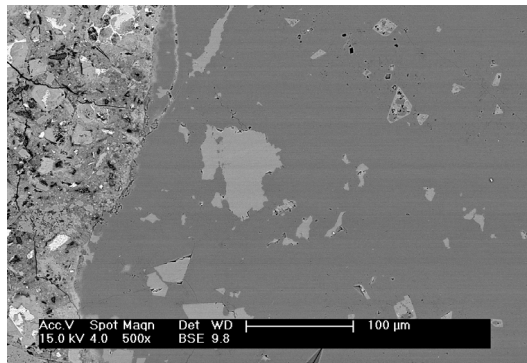


Figure 12: Sandstone with no signs of reaction (dark grey mineral = quartz, light grey mineral = feldspar). Concrete produced with aggregate B.